The Cerebellum (2019) 18:500–510
https://doi.org/10.1007/s12311-019-01015-7

ORIGINAL PAPER

Neural Scaffolding as the Foundation for Stable Performance of Aging Cerebellum

Pavel Filip[1,2] · Cécile Gallea[3] · Stéphane Lehéricy[3] · Ovidiu Lungu[4,5] · Martin Bareš[2,6]

Published online: 2 March 2019

Abstract

Although recently conceptualized as a neural node essential for a vast spectrum of associative and cognitive processes, the cerebellum has largely eluded attention in the research of aging, where it is marginalized mainly to structural analyses. In the current cross-sectional study of 67 healthy subjects of various ages (20 to 76 years), we sought to provide a comprehensive, multimodal account of age-related changes in the cerebellum during predictive motor timing, which was previously shown to engage this structure. We combined behavioral assessments of performance with functional MRI and voxel-based morphometry using an advanced method to avoid cerebellar deformation and registration imprecisions inherent to the standard processing at the whole-brain level. Higher age was surprisingly associated with stable behavioral performance during predictive motor timing, despite the massive decrease of infratentorial gray matter volume of a far higher extent than in the supratentorial region, affecting mainly the posterior cerebellar lobe. Nonetheless, this very area showed extensive hyperactivation directly correlated with age. The same region had decreased connectivity with the left caudate and increased connectivity with the left fusiform gyrus, the right pallidum, the hippocampus, and the lingual gyrus. Hence, we propose to extend the scaffolding theory of aging, previously limited mainly to the frontal cortices, to include also the cerebellum, which is likewise suffering from atrophy to a far greater extent than the rest of the brain and is similarly counteracting it by bilateral hyperactivation.

Keywords Cerebellar aging · fMRI · Functional connectivity · Voxel-based morphometry

✉ Pavel Filip
pvlfilip@gmail.com

[1] Center for Magnetic Resonance Research (CMRR), University of Minnesota, Minneapolis, MN, USA

[2] First Department of Neurology, Faculty of Medicine, University Hospital of St. Anne, Masaryk University, Brno, Czech Republic

[3] Institut du Cerveau et de la Moelle épinière—ICM, Centre de NeuroImagerie de Recherche, Sorbonne Université UMR S1127, Inserm U1127, CNRS 7225, Paris, France

[4] Department of Psychiatry, Université de Montréal, Montréal, Québec, Canada

[5] Functional Neuroimaging Unit, Research Center of the Geriatric Institute affiliated with the Université de Montréal, Montréal, Québec, Canada

[6] Department of Neurology, School of Medicine, University of Minnesota, Minneapolis, MN, USA

Abbreviations

MRI	Magnetic resonance imaging
fMRI	Functional magnetic resonance imaging
VBM	Voxel-based morphometry
BOLD	Blood-oxygen-level dependent

Introduction

Facing the substantially increasing proportion of elderly in the population, the development of appropriate preventive measures and interventions together with the struggle to truly understand the mechanisms of aging has become one of the core pursuits of the medical science. Indeed, the widespread alterations in the cognitive and psychomotor performance in various domains [1, 2] interfere with not only complex activities but also routine, daily tasks, generating major costs for health and social services [3]. Modern theories about the processes underlying these

declines share the view that the aging-associated neural insults are partially compensated by continuous functional reorganization, reflected in the difference in brain activation patterns in older adults, especially in the form of increased bilateral activation in the prefrontal cortices [4, 5]. Nonetheless, the pervasive evidence in the psychological, behavioral, and imaging studies, despite greatly advancing our understanding and knowledge of the basic concepts of aging, keeps revolving around the cerebral cortex, leaving the cerebellum outside the attentional focus and, in imaging studies, often even outside the scanning target. However, while classically conceptualized as a neural node engaged in motor coordination, the cerebellum has recently been emerging as a structure of interest in a vast spectrum of associative and cognitive processes [6] and various perhaps even counterintuitive diseases devoid of the traditional clinical cerebellar symptoms [7, 8], making it a critical area also for the research into aging [9]. A large body of literature has focused on the cerebellar morphology, reporting decreased both total [10, 11] and regional cerebellar volumes [12]. In parallel, several fMRI and resting state fMRI studies, though targeting rather supratentorial (cerebral, over the tentorium cerebelli) structures, have also highlighted the potential role of the cerebellum in aging [13, 14], showing considerable disruption of motor and cognitive processing [9, 15].

The aim of the current cross-sectional study was to provide a comprehensive, multimodal account of the age-related changes in the cerebellum, with specific focus on its role in the model of predictive motor timing, i.e., the analysis of environmental factors to estimate the probable future state of the surroundings as a prerequisite for eventual preemptive actions (e.g., preparation of adequate limb position to catch a moving object). A close association of this function with dominantly posterior cerebellum was previously established both in healthy subjects [16] and in various disorders [17, 18], an area closely related to executive functions and cognition in general according to multiple clinical and imaging studies [6, 19]. Ergo, as the eminent orientation of this project towards the cerebellum clearly required more specific methods devoid of errors of cerebellar alignment and normalization inherent to the analyses at the level of the whole brain, we intended to capitalize on the benefits of the SUIT toolbox [20, 21] with the ability to isolate cerebellar structures, and relevant probabilistic maps to achieve valid assignment of functional activations to specific cerebellar lobules and nuclei. Our preliminary hypothesis anticipated an age-related (i) decrease in the behavioral performance, (ii) compensatory response of various cerebellar areas and abnormal functional connectivity with regions implicated in predictive timing [16], and (iii) overlap of the structural and functional changes in the cerebellar lobules reflecting degenerative processes.

Materials and Methods

Subjects

A total of 67 healthy volunteers (36 women, mean age 45.61; SD 14.63; range 20 to 76, with rather even distribution; age 20–30, 10 subjects; 30–40, 17 subjects; 40–50, 12 subjects; 50–60, 14 subjects; 60–70, 11 subjects; and age group 70+, 3 subjects) were recruited at the First Department of Neurology, Masaryk University, Brno (55 subjects) and at the University of Minnesota (12 subjects) to participate in this study. All subjects provided written informed consent and underwent safety screening before MRI scanning; no structural pathology was found in their anatomical MRI scans. Individuals with MRI contraindications, comorbid psychotic or neurological disorder, obvious cognitive deficit (MMSE < 27 or subjective cognitive impairment), or evidence of significant vascular or space-occupying lesions in MRI scans were excluded from the study. All participants were right-handed [22]. The study was approved by the Institutional Review Board of the University Hospital of St. Anne (Brno, Czech Republic) and by the Institutional Review Board of the University of Minnesota (Minneapolis, USA).

Design of the Experimental Task

The study used the very same predictive timing task as implemented in our previous projects, which had been extensively tested both in healthy subjects [16], patients with dominantly cerebellar deficits [23], disorders with probable affection of the cerebellum [17, 24] and even psychiatric patients [25] to test for eventual cerebellar affections. It had been shown to entrain mainly the posterior cerebellum and to a certain extent the middle temporal gyrus, putamen, and occipital areas [16]. It required a single press of a key to launch a projectile vertically from the right lower corner of the screen to intercept a target moving from the left side of the screen to the right upper corner with varying speed (slow, medium, high), movement types (stable, acceleration, deceleration) and angles (3 possible angles) (see Fig. 1) to provide 27 different combinations of movement parameters with the aim of moderating or completely abolishing the possible learning effect. The participants had to follow the moving target at all times. The task was presented using LabVIEW 6.1 (National Instruments, Austin, TX, USA) interface.

The whole experiment consisted of a training session performed already during scanning in the MRI system to familiarize the subjects with both the task at hand and with MRI environment and the main task, which was analyzed here. The main task was organized into 6 blocks, each consisting of 54 trials, with a pseudo-randomized sequence of target movement combinations for a total of 324 trials (each movement parameter combination was presented 12 times in total). Each

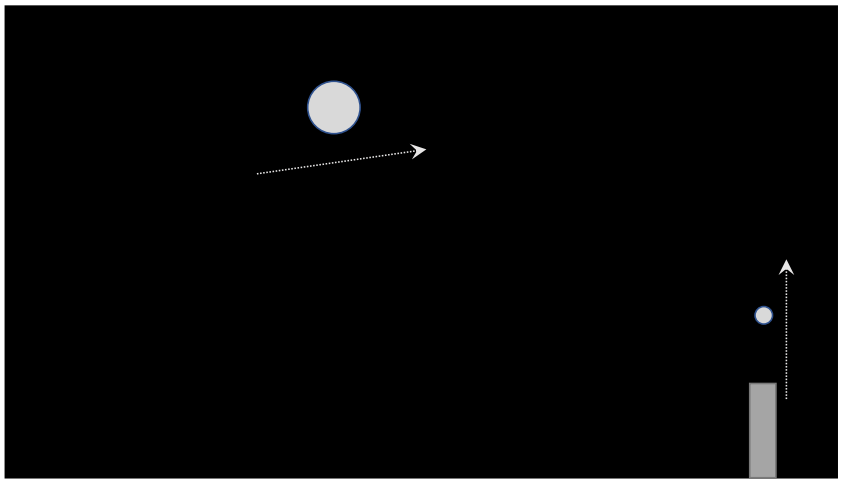

Fig. 1 The experimental task—schematics. The circular target moves from the left side of the screen to the upper right corner—the interception zone. The figure also contains a projectile just fired from the lower right corner of the screen vertically at a constant speed to intercept the target

block contained a balanced presentation of various stimuli to prevent the repetition of the same kinetic parameters of the target in consecutive trials to avoid learning effects. The average duration of one trial was 3.5 s and the whole acquisition (including the training session, the main session with 20-s breaks to minimize cognitive fatigue, and the acquisition of anatomical scans) was about 50 min.

MRI Data Acquisition

MRI scanning was performed using a 3-Tesla whole-body MRI scanner (MAGNETOM Trio, Siemens Medical Systems, Erlangen, Germany) and a 1.5-Tesla whole-body MRI scanner (Siemens Symphony with Numaris 4, Siemens Medical Systems, Erlangen, Germany) at the University of Minnesota and at the Imaging Department of the University Hospital of St. Anne, Brno, respectively, necessitating adequate measures in the imaging data analysis, which accounted for the use of different fields by including the MRI system as a nuisance variable in the second-level analysis model.

At the beginning, high-resolution anatomical T1-weighted images were acquired with the following parameters: at the 3-T system, fast low angle shot magnetic resonance imaging (FLASH) sequence (repetition time (TR) = 13 ms, echo time (TE) = 4.92 ms, flip angle (FA) = 25°, voxel size 1 × 1 × 1 mm, 160 sagittal slices, matrix 256 × 256 × 160), and at the 1.5-T system, magnetization-prepared rapid gradient echo (MPRAGE) sequence (TR = 1.7 s, TE = 3.93 ms, in-plane voxel size 0.96 × 0.96 mm, 160 sagittal slices, slice thickness 1.17 mm, matrix 256 × 256 × 160). Afterwards, whole-brain fMRI was performed with echo-planar imaging sequence with the following parameters: at the 3 T system, TR = 2.0 s, TE = 30 ms, FA = 75°, voxel size 3 × 3 × 3 mm, 30 sagittal slices, field of view 192 × 192 mm, and total number of volumes 556 and at the 1.5 T system, TR = 2.3 s, TE = 35 ms, FA = 90°, in-plane voxel size 3.44 × 3.44 mm, 28 sagittal slices, slice thickness = 4.40 mm, field of view 220 × 180 mm, and total number of volumes 490.

Analysis of Demographic and Behavioral Data

Firstly, equivalence analysis (Schuirmann's two one-sided test [26]) was used to confirm the absence of significant differences in basic demographic parameters (age, gender) between the subjects enrolled in Minneapolis, USA, and the subjects enrolled in Brno, Czech Republic. The aim was to verify the absence of substantial demographic divergences, with 10-year and 25% mean difference considered clinically relevant for the age and the gender, respectively.

The primary variable of interest was the hit ratio in different speeds and types of movements. Similar to the previous analyses, the angle was excluded, since it was proven of no effect on the success rate [27]. We determined the mean hit ratio of each participant for every movement type of interest in order to use parametric statistical analysis. Furthermore, we were interested in the temporal characteristics of errors, differentiating between early errors (EE) and late errors (LE) (the subject pressed the button too early or too late, respectively). The correlation of age and hit ratios in individual movement types was evaluated using Pearson's correlation coefficient. Student's *t* test was used to compare the EE and LE occurrence. And finally, although our previous papers found no learning effect in a basic analysis comparing the hit ratio in the first 3 blocks and the second 3 blocks of the experiment [24, 27], we added a more complex analysis of covariance, distinguishing the 6 blocks of the main task as categorical variables, with the age as covariate and the following dependent variables: hit ratios and quantification of temporal precision (i.e., absolute time differences between the ideal time of projectile release to intercept the moving target and the actual time the subject pressed the button to fire the projectile). All the analyses were performed using Statistica 13 (Statsoft Inc., Oklahoma, USA).

Analysis of MRI Data

MRI data were pre-processed and analyzed using SPM8 (Wellcome Department of Cognitive Neurology, London, UK) implemented in Matlab R2017b (Mathworks Inc., Natick, MA, USA). The fMRI images were realigned to correct for subject's head movements; the threshold of a 3-mm shift in any direction or 3° rotation was not exceeded by any subject. Afterwards, interpolation in time was performed. As the primary aim of our study was heavily oriented on the cerebellum, the further workflow utilized the automated nonlinear normalization methods of the SUIT toolbox and the spatially unbiased atlas template of the cerebellum [21] to achieve a more accurate subject alignment in this region than feasible with the whole-brain level methods. The isolated mask of the cerebellum created by the toolbox was manually corrected in each subject using MRIcron and the anatomical image was normalized to the SUIT template using nonlinear deformation.

First, we studied the influence of age on structural cerebellar changes. Anatomical MRI data were segmented using the algorithm implemented in the SUIT toolbox and the gray matter (GM) images were normalized to the SUIT template. The same manually corrected cerebellar masks as described above were then used to reslice the segmentation map into the SUIT atlas space. In the final step, the resulting GM probability images were smoothed with a Gaussian kernel of 8 mm full-width at half-maximum. Finally, regression analysis of age-related differences was performed, with the gender, hit ratio, and MRI system as the nuisance variables. Moreover, the individual infratenorial intracranial volumes were included in the statistical model to account for general volume differences.

Second, we studied the influence of age on task-related activations and their spatial overlap with age-related structural changes. The first-level general linear model of BOLD activations was defined using an event-related design to model the effect of the movement parameters in the task, with the onset at the moment the circular moving target emerged at the left side of the screen, and the end at the time the subject pressed the key to fire the projectile. The individual design matrix for each subject consisted of speed (slow, medium, high) and movement type (acceleration, deceleration, stable speed), with the head movements in all directions as the nuisance covariates, providing nine contrast maps. These functional data were resliced based on the deformation of the individual anatomical image to the SUIT template, thus optimizing the spatial accuracy of the cerebellar activations. Only at this point were the functional data spatially smoothed (isotropic Gaussian kernel of 8 mm full-width at half-maximum) to prevent the spread of the activation from the visual cortex to the infratentorial area. The images were resampled to a final size of $3 \times 3 \times 3$ mm^3 and high-pass filtered with a Gaussian kernel filter of 128 s. The results were then submitted to the second-level full factorial design (3×3) with the following factors: speed (3 types) and movement type (3 types), and the age as a covariate of interest. Furthermore, hit ratio, gender, and importantly the MRI system used to acquire the images were included as the nuisance variables to control for the effects associated with these parameters and the use of two different scanning devices. In an additional step to define the overlap between the age-related activation changes and the GM volume loss, we used the significant clusters of cerebellar atrophy from the structural analysis as a mask for the above-stated second-level analysis results.

Third, we studied the influence of age on task-related connectivity. The connectivity (psychophysiological interaction or PPI [28]) analysis was performed at the level of the whole brain to test the hypothesis of changes in the network associated with predictive timing. Ergo, the preparatory phase of the functional data included realignment, co-registration of functional and anatomical images, interpolation in time, followed by the standard spatial normalization into the stereotactic Montreal Neurological Institute (MNI) space (without the use of the SUIT toolbox), and spatial smoothing and high-pass filtering with the same parameters as stated above. The first-level model used as the basis for the PPI analysis corresponded to the above-described design for cerebellar analysis, with the individual design matrix for each subject consisting of speed (slow, medium, high) and movement type (acceleration, deceleration, stable speed), and the head movements in all directions as the nuisance covariates. In this model, we analyzed the connectivity of cerebellar seeds using PPI models. Specifically, AAL-defined cerebellar lobules arising as the most prominent ones (most significant age-related differences) in the activation and structural analysis (see below), i.e., left crus I, right crus I, left crus II, right crus II, and right lobule VI, were used. The time course of individual seeds was extracted as the average over these atlas-defined cerebellar lobules of interest. The first-level PPI models at the individual level included the extracted time series, the task regressor (high vs. slow speed), and the PPI regressor (product of the task regressor and the deconvolved extracted time series), generating three individual PPI t-contrasts, which were submitted to the second-level regression analysis with age as a covariate and hit ratio, gender, and MRI system as the nuisance variables. The movement type was not included in the connectivity analysis due to its lower signature in the activation analysis (see the "Results" section).

Probabilistic atlas defined by Diedrichsen [20] implemented in the SPM Anatomy toolbox [29] was used to identify the activation clusters in the SUIT space in the cerebellum and the Automated Anatomical Labeling (AAL) atlas database [30] was utilized in the connectivity analysis encompassing the whole brain.

Statistical Thresholds

In the activation analysis and VBM, results were considered significant at $p < 0.05$, family-wise error (FWE)–corrected for multiple comparisons at the voxel level (with the cluster threshold of 50 and 200 contiguous voxels for the activation analysis and VBM, respectively). In the PPI analysis, we adopted a less-stringent threshold of $p < 0.05$, FWE-corrected for multiple comparisons at the cluster level (voxel-wise threshold of $p < 0.001$, uncorrected, small volume correction). And finally, the behavioral results utilize the significance level of $p < 0.01$.

Results

The equivalence analysis of demographic variables in the first step using two one-sided test revealed that the two samples were significantly equivalent in age ($p = 0.034$) and gender ($p = 0.001$), with no difference between the subjects enrolled in Minneapolis and in Brno. Ergo, the subjects were processed as a single cohort in all the subsequent analyses.

Behavioral Results

The initial analysis of pooled data from all participants provided the average hit ratio of 0.4354 (SD = 0.0853), with the average EE ratio of 0.2920 (SD = 0.0609) and the average LE ratio of 0.2726 (SD = 0.0818). No difference was found between the relative occurrence of the errors of different types (EE vs. LE, 51.7% vs. 48.3%, respectively) ($p > 0.05$). Interestingly though, the correlation analysis revealed virtually no effect of aging on the behavioral performance in any of these parameters ($r_{\text{age-hit}} = -0.031$, $r_{\text{age-EE}} = -0.096$, $r_{\text{age-LE}} = 0.103$; $p > 0.2$ for all analyses). The performance based on the rate of the speed did not correlate with age ($r_{\text{age-slow}} = 0.133$, $r_{\text{age-medium}} = -0.068$, $r_{\text{age-high}} = -0.136$; $p > 0.2$ for all analyses). However, the success rate was inversely correlated with age for trials where stimuli moved on the screen with different acceleration rates ($r_{\text{age-acceleration}} = -0.534$; $p < 0.0001$), and, conversely, individuals with higher age were able to cope with stable speed slightly better than the younger participants ($r_{\text{age-stable speed}} = 0.315$; $p = 0.001$). The extent of correlation between performance in decelerated trials and age did not reach the significance threshold ($r_{\text{age-deceleration}} = 0.120$; $p > 0.20$). Furthermore, no learning effect was found in any of the parameters in the ANCOVA analysis comparing the first and the second half of the experiment with the age as a covariate: hit ratio ($F = 0.452$, $p > 0.2$) and absolute time difference between the ideal and the actual time of button press ($F = 0.515$, $p > 0.2$).

Structural Analysis

The analysis of the association between age and GM volume revealed a significant negative correlation in the infratentorial area ($r = -0.620$; $p < 0.0001$), but only borderline results for the whole brain ($r = -0.268$; $p = 0.028$), resulting in a steep decrease in the ratio of the infratentorial GM volume to the whole intracranial GM volume (see Fig. 2).

Figure 3A and Table 1 illustrate the patterns of larger cerebellar atrophy associated with higher age. The profile of atrophy was more pronounced in the posterior cerebellum (bilateral crus I, left crus II, right lobule VI, and right lobule and vermis IX); the anterior cerebellum was affected only slightly (left lobule V). No age-related GM volume increase was found.

Activation Analysis

The results of the 3 × 3 ANOVA (speed × movement type) with age as the covariate of interest were as follows:

1. *Main effect of speed*: Higher speed of the target was closely associated with the cerebellar activity in the posterior cerebellum, specifically in both lobules VI (Fig. 3B, Table 1).
2. *Main effect of movement type*: The changes in movement type were associated with a higher activation in the posterior cerebellum, specifically the vermis VIIIa and the left hemispheric lobule VI) (Fig. 3C, Table 1).
3. *Interaction of speed and movement type*: No activations surpassed the statistical threshold.
4. *Positive association between age and activation (directly proportional activation)*: Higher age was related with an increased activation dominantly in the posterior cerebellum, encompassing both crura I and II, to a far lesser extent in the anterior cerebellum (right lobule V) (Fig. 3D, Table 1).
5. *Negative association between age and activation (inversely proportional activation)*: Younger subjects activated a small area in the anterior cerebellum (specifically lobule IV) more than their older counterparts (Fig. 3E, Table 1).
6. *Overlap between the GM volume loss and the activation proportional to age*: Both crura I and the left crus I showed a marked hyperactivation even though significantly affected by GM atrophy (Table 1).

Connectivity Maps

The seeds for the PPI analysis were localized in the areas with most significant age effect, both from VBM and the activation

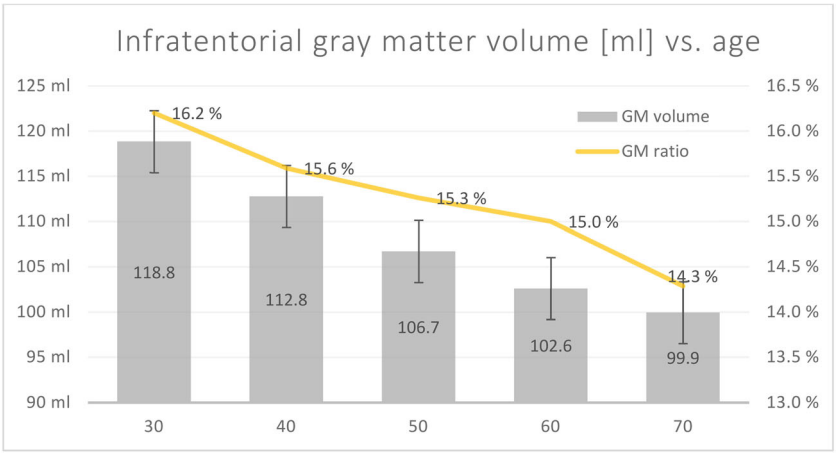

Fig. 2 Reduction of the infratentorial GM volume and the ratio of infratentorial GM volume to the intracranial GM volume. The *x*-axis depicts age groups, the left and right axes denote infratentorial GM volume and the ratio of the infratentorial to the intracranial GM volume as percentage, respectively. Error bars for GM volume columns represent standard errors

analysis: left crus I, right crus I, left crus II, right crus II, and right lobule VI.

1. *Seed in the left crus I*: Higher age was associated with decreased connectivity mainly to the left caudate and in lesser extent also to the right caudate (Fig. 4A, Table 2). The inverse contrast failed to yield any significant clusters at the predetermined threshold.
2. *Seed in the right crus I*: Once again, higher age was associated with decreased connectivity to the left caudate. On

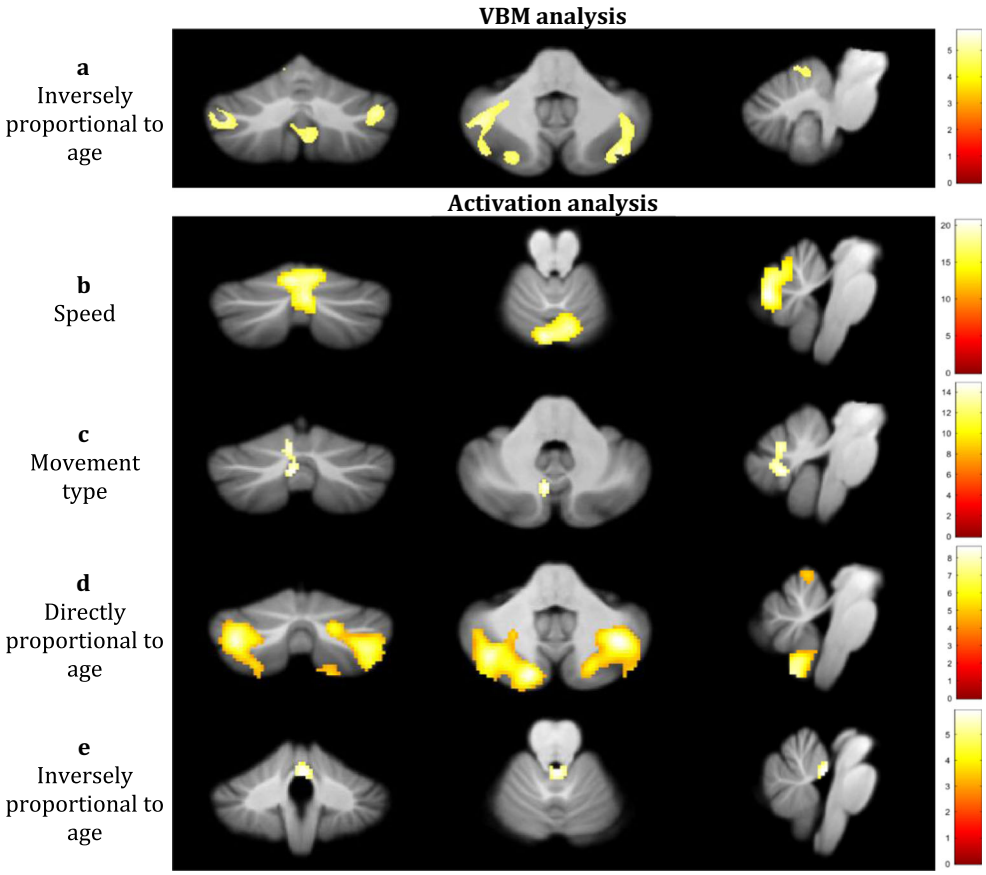

Fig. 3 Results of the 3 × 3 ANOVA with the age as the covariate of interest ($p < 0.05$, FWE-corrected at the voxel level), in frontal, axial, and sagittal views in SUIT space. **a**—VBM results (threshold $T = 4.43$) showing reduced GM volume in higher age (i.e., older individuals) dominantly in the posterior cerebellum. **b**—main effect of speed (*F*-contrast) (threshold $F = 12.15$), with increased activation in the posterior cerebellum during higher speeds. **c**—main effect of movement type (*F*-contrast) (threshold $F = 12.15$), yielding increased activation in the vermis VIIIa and left hemispheric lobule VI. **d**—vast bilateral hyperactivation of the posterior cerebellum associated with higher age (threshold $T = 4.33$). **e**—area in the lobule IV activated less in older subjects (threshold $T = 4.33$). Conventions for the laterality were used where the right side in the figure corresponds to the right cerebellum. See Table 1 for detailed statistical results and anatomical localization of clusters

Table 1 Anatomical localization of clusters in the activation and VBM analysis focused exclusively on the cerebellum

Cluster no.	Structure (cerebellar lobules)			Volume (in voxels)	*p* value (FWE)	*F*-score of local max	MNI coordinates of local maxima		
Activation—main effect of speed									
1	R VI	Hem	23.0%	645	< 0.001	20.66	2	− 76	− 29
	R VI	Verm	18.2%						
	L VI	Verm	14.7%						
	L VI	Hem	12.5%						
Activation—main effect of movement type									
1	L VIIIa	Verm	44.3%	72	0.005	14.86	− 6	− 68	− 37
	L VI	Hem	20.0%						
Cluster no.	Structure (cerebellar lobules)			Volume (in voxels)	*p* value (FWE)	*T*-score of local max	MNI coordinates of local maxima		
Activation directly proportional to age									
1	R VIIa, crus I	Hem	41.4%	2246	< 0.001	8.60	36	− 62	− 39
	R VIIa, crus II	Hem	16.9%						
	R IX	Hem	10.0%						
2	L VIIa, crus I	Hem	40.2%	1694	< 0.001	8.34	− 14	− 82	− 39
	L VIIa, crus II	Hem	39.1%						
3	R V	Hem	80.5%	93	< 0.001	6.45	12	− 52	− 9
4	L VI	Hem	85.2%	59	0.009	4.78	− 22	− 48	− 25
	L V	Hem	14.8%						
Activation inversely proportional to age									
1	R IV	Hem	56.1%	55	< 0.001	5.93	2	− 44	− 21
	L IV	Hem	36.6%						
GM volume inversely proportional to age									
1	L VIIa crus I	Hem	58.9%	2482	0.003	5.31	− 37	− 58	− 36
	L VIIa, crus I	Hem	25.3%						
2	R VIIa crus I	Hem	85.2%	2403	0.003	5.36	40	− 58	− 34
	R VI	Hem	13.5%						
3	R IX	Hem	59.8%	734	0.002	5.45	4	− 63	− 50
	L VIIIb	Verm	13.4%						
	R IX	Verm	13.2%						
4	L V	Hem	66.0%	356	0.001	5.75	− 17	− 57	− 14
	L VI	Hem	34.0%						
Overlap between the GM volume loss and the activation proportional to age									
1	R VIIa, crus I	Hem	96.7%	173	< 0.001	8.50	38	− 62	− 39
2	L VIIa, crus II	Hem	52.2%	151	< 0.001	8.16	− 38	− 72	− 41
	L VIIa, crus I	Hem	47.6%						

Clusters are significant at $p < 0.05$, FWE-corrected for multiple comparisons at the voxel level (with the cluster threshold of 50 and 200 contiguous voxels for the activation analysis and VBM, respectively). Only cerebellar lobules covering at least 10.0% of the respective activation cluster are listed in the table. *L*, left; *R*, right; *Hem*, hemisphere; *Verm*, vermis; *MNI*, Montreal Neurological Institute; *FWE*, family-wise error

the other hand, they had increased connectivity to several areas, including the cerebellar lobules IV, V, left lingual and fusiform gyri, and the right hippocampus (Fig. 4B, Table 2).

3. *Seed in the left crus II*: No significant connectivity differences associated with age were found.
4. *Seed in the right crus II*: Higher age was associated with decreased connectivity to the left angular gyrus (Fig. 4C, Table 2). The reverse contrast revealed no significant differences.
5. *Seed in the right lobule VI*: Similar to the connectivity of both the left and the right crus I, the older subjects had significantly decreased connectivity to the left caudate. On the other hand, they showed increased connectivity to the left fusiform gyrus and the right pallidum (Fig. 4D, Table 2).

Discussion

The extent to which the functional capacity of the cerebellum is disrupted in older age remains notably underexplored,

despite the mounting evidence on progressive changes, possibly detrimental to its performance [9]. We found well-preserved behavioral performance in predictive temporal estimation associated with vast hyperactivation of the posterior cerebellum, despite the atrophy of this area, corroborating previous reports of marked age-related alterations. Our findings provide a novel, multimodal insight on the aging cerebellum escaping the trend of functional performance decline in the supratentorial region.

Nonetheless, our promising findings of surprisingly stable performance in higher age compared with younger age group in an excessively demanding task able to distinguish even slight cerebellar abnormities [17, 24, 27] must be put into the context of other studies reporting reduced functional outcomes in tasks dependent on the cerebellum in older individuals [31, 32]. Indeed, we cannot truly escape the grim truth hidden behind the strongly negative correlations of cerebellar volume with the advancing age, very much in keeping with quite extensive body of research [11, 33] and similar in magnitude only to the prefrontal cortex and hippocampus [33]. A limitation of the present study is probably an insufficient coverage of the relevant high-age spectrum in our cohort, which could explain why we did not find the reported nearly quadratic rate of cerebellar volume decrease in elderly individuals [34]. Despite this fact, we could corroborate the findings of the dominant impact of aging on posterior lobes, mainly crus I, and partly also the anterior cerebellum [12]. Our study also complements the previously reported association of age with the atrophy of the vermis [10, 35].

Regarding our main findings, the hyperactivation in both cerebellar lobes VII is of plausible association with the presented task itself, as these areas have been repeatedly implicated in spatial processing and executive functions (for review, see [36]). Of further relevance is the emergence of lobule IX, a region related rather to sensorimotor processing [6]. All in all, the vast bilateral hyperactivation in the posterior

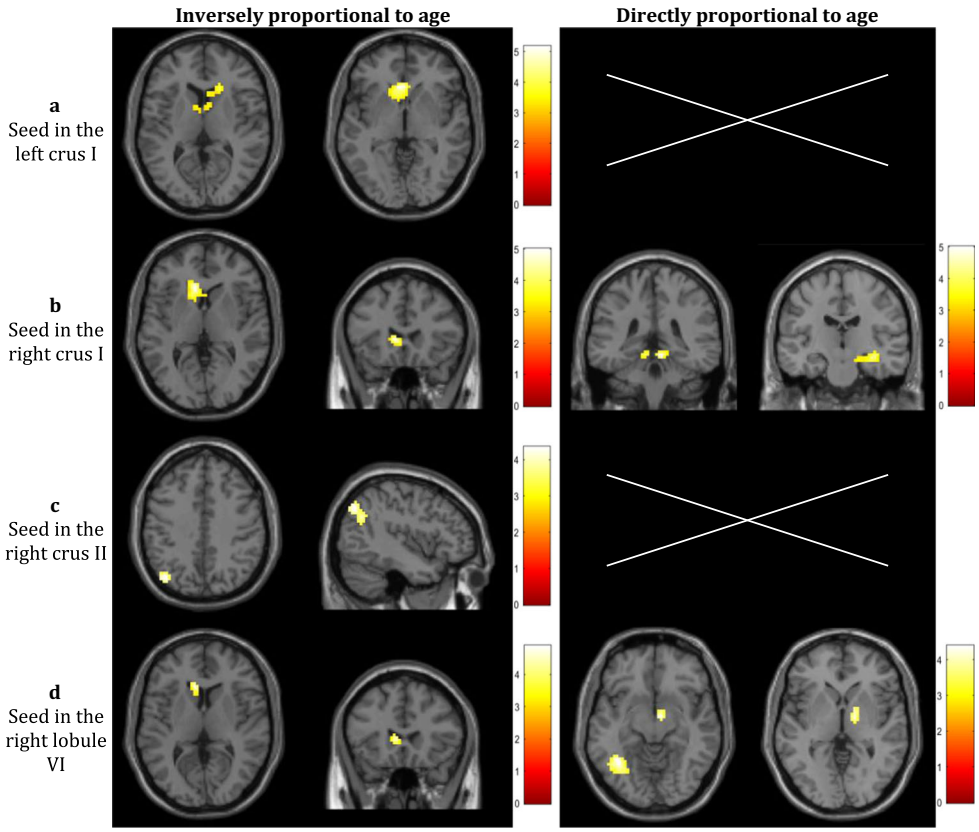

Fig. 4 Results of the connectivity analysis ($p < 0.05$ FWE-corrected at the cluster level) at the cluster level ($p < 0.001$ uncorrected at the voxel level; threshold $T = 3.14$). White crosses in the results denote the absence of any statistically significant results. **a**—*Seed in the left crus I*: reduced connectivity mainly to the left caudate, to a lesser extent to the right caudate in higher age. No connectivity increase associated with higher age was found. **b**—*Seed in the right crus I*: again, reduced connectivity to the left caudate in higher age. Increased connectivity to the anterior cerebellum and the right hippocampus. **c**—*Seed in the right crus II*: reduced connectivity to the left angular gyrus in subjects with higher age. No connectivity increase associated with higher age was revealed. **d**—*Seed in the right lobule VI*: also, decreased connectivity to the left caudate in older subjects. The reverse contrast yielded a significant increase in connectivity to the left fusiform gyrus and the right pallidum. Conventions for the laterality were used where the right side in the figure corresponds to the right side in the scanned area. See Table 2 for detailed statistical results and anatomical localization of clusters

Table 2 Anatomical localization of clusters in the connectivity analysis

Anatomical regions	Brodmann area or lobule in the cerebellum	Side	Volume (in voxels)	*p* value (SVC)	*T*-score of local max	MNI coordinates of local maxima		
Seed in the left crus I								
Inversely proportional to age								
Caudate		L	264	< 0.001	5.17	− 6	16	1
Caudate		R			4.06	18	20	13
Seed in the right crus I								
Inversely proportional to age								
Caudate		L	86	< 0.001	5.00	− 9	16	4
Directly proportional to age								
Lingual gyrus	BA30	R	55	< 0.001	4.92	9	− 37	− 11
Cerebellum	Lobule IV, V	L	71	< 0.001	4.81	− 9	− 48	− 14
Hippocampus		R	101	< 0.001	4.36	33	− 16	− 14
Fusiform gyrus	BA 37	L	55	0.001	4.20	− 39	− 64	− 14
Seed in the right crus II								
Inversely proportional to age								
Angular gyrus	BA 39	L	99	< 0.001	4.35	− 42	− 70	40
Seed in the right lobule VI								
Inversely proportional to age								
Caudate		L	57	< 0.001	4.89	− 9	16	7
Directly proportional to age								
Fusiform gyrus	BA 37	L	124	< 0.001	4.38	− 36	− 55	− 14
Pallidum		R	58	< 0.001	4.32	15	− 1	− 2

Clusters are significant at $p < 0.05$, FWE-corrected for multiple comparisons at the cluster level (voxel-wise threshold of $p < 0.001$, uncorrected, small volume correction). *L*, left; *R*, right; *BA*, Brodmann area; *MNI*, Montreal Neurological Institute; *SVC*, small volume correction; *FWE*, family-wise error

cerebellum associated with increased age provides evidence for the general concept delineated in the previous neuroimaging research, which has long revealed that older adults exhibit different brain activation with a bilateral increase in the prefrontal cortices [5, 37]. Interestingly, age-related dysfunction of the cerebellum has been largely marginalized in this research area, with the majority of literature being oriented on morphology [9]. Rather scarce fMRI reports implicated both increased [5, 31, 38] and to a far lesser extent decreased [39, 40] activation in the cerebellum associated with aging in various tasks, but generally, as a complement to the main supratentorial finding, giving an edge to our neuroimaging analysis devoid of cerebellar deformations and registration imprecisions inherent to the processing at the level of the whole brain. The normalization to the high-resolution spatially unbiased SUIT template of the cerebellum implemented in this project allows for higher confidence in our findings, thanks to the reduced inter-subject spatial variance and more precise probabilistic atlas-based localization. Moreover, the decreased connectivity of these very cerebellar regions, exhibiting a seemingly counterintuitive combination of hyperactivation and atrophy, to various structures conforms with the generally accepted overall pattern of decreased functional connectivity associated with increasing age [14]. The repeated emergence of hypoconnectivity to the left caudate from multiple areas, specifically both crura I and the right lobule VI, is of much interest. It not only complements previous reports of decreased cerebellar connectivity to the basal ganglia in aging [39] but it also partly builds upon our previous analysis of structures engaged in the very same task focusing on predictive motor timing [16], where caudate emerged as a major node participating in success and failure assessment. No age-related connectivity changes have been found in the other supratentorial structures previously implicated in this task (middle temporal gyrus, putamen, and occipital lobe) [16]. All in all, the combination of this connectivity decrease with increased connectivity to several regions responsible for visuospatial attention [41] and neural pathways related to recognition and short-term memory points to possible compensatory efforts of the aging cerebellum and its network. However, further components, possibly even inherent to the task itself (e.g., different strategy in close association with age), may well have contributed to the absence of correlation between the age and the performance, calling for similarly designed studies focusing on different cerebellar functions. Furthermore, even though it is tempting to attribute all the

BOLD changes purely to hypothesized underlying neuronal alterations, there is a non-negligible association of vascularity, hemodynamic and vasomotor response with age [42, 43] potentially confounding all the fMRI and connectivity studies of aging, an issue, which definitely requires further extensive research in the years to come. A further limitation to this study is the absence of extensive neuropsychological battery and hence the possibile inclusion of subjects with initial stages of cognitive disorders, even though of low risk considering the normal MMSE levels and no subjective complaints in this area. And lastly, one of the major limitations of the presented study is the possible interference of the use of two MRI scanners with different strengths of magnetic field, despite the inclusion of this parameter to the statistical model.

All in all, our study is the first to provide a multimodal account of aging specifically in the cerebellum, including a behavioral perspective, morphological, activation, and connectivity aspects, all in one group of subjects. The bilateral hyperactivation of cerebellar areas most affected by atrophy leading to a behavioral outcome comparable to younger subjects, despite the decreased connectivity to areas relevant for the task, is not unlike the processes described in the frontal cortex in aging—likewise suffering from atrophy in far higher extent than the rest of the brain and likewise answering with increased bilateral activation to compensate for age-related insults. This very area was the focus of the landmark paper introducing the scaffolding theory of aging and cognition [44]. Scaffolding is one of the basic concepts of learning envisaged as selective honing of the initial, dispersed network activated in early processes to the most specific and optimal circuit to mediate efficient functions. And aging, associated with gradual encroachment of pathological processes diminishing the neurobiological efficiency of these optimized pathways, seems to lead to re-erection of the scaffolds previously acquired during early learning or the recruitment of newly established scaffolds to compensate for the damaged or lost networks in the frontal cortex. Nonetheless, this may well be the case also for the cerebellum that, utilizing its innate learning skills [45], recruits further areas to compensate for the age-related alterations, even increasing the communication with supratentorial regions previously non-dominant in the specific task, to preserve the task performance and behavioral outcomes. Nonetheless, whether this age-related hyperactivation is limited to the cognition-related posterior part of the cerebellum, which boasts extensive connections to associative cortices [46], or it affects also the anterior cerebellum, remains to be established using appropriate experiment designs.

The picture emerging here represents a refinement and synthesis of ideas appearing in the recent years and their application to the often-overlooked cerebellum, extending the scaffolding theory of aging to this remarkable neuronal machine. In times with dire need to understand the precise neurobiological mechanisms of aging, together with the search for possible methods for preservation and enhancement of central nervous system function in growing proportion of elderly population, our results provide novel insights in the reorganization of cerebellar activity and networks associated with aging.

Acknowledgments The authors are grateful to the patients and their families for their support of this research.

Funding This work was supported by the EU H2020 Marie Skłodowska RISE project #691110 (MICROBRADAM).

Compliance with Ethical Standards The study was approved by the Institutional Review Board of the University Hospital of St. Anne (Brno, Czech Republic) and by the Institutional Review Board of the University of Minnesota (Minneapolis, USA).

Conflict of Interests There are no potential conflicts of interests regarding this paper and no financial or personal relationships that might bias this work.

References

1. Seidler RD, Bernard JA, Burutolu TB, Fling BW, Gordon MT, Gwin JT, et al. Motor control and aging: links to age-related brain structural, functional, and biochemical effects. Neurosci Biobehav Rev. 2010;34(5):721–33.
2. Salthouse TA. Selective review of cognitive aging. J Int Neuropsychol Soc. 2010;16(5):754–60.
3. Harper S. Economic and social implications of aging societies. Science. 2014;346(6209):587–91.
4. Naccarato M, Calautti C, Jones PS, Day DJ, Carpenter TA, Baron JC. Does healthy aging affect the hemispheric activation balance during paced index-to-thumb opposition task? An fMRI study. Neuroimage. 2006;32(3):1250–6.
5. Mattay VS, Fera F, Tessitore A, Hariri AR, Das S, Callicott JH, et al. Neurophysiological correlates of age-related changes in human motor function. Neurology. 2002;58(4):630–5. https://doi.org/10.1212/WNL.58.4.630.
6. Stoodley CJ, Schmahmann JD. Functional topography in the human cerebellum: a meta-analysis of neuroimaging studies. Neuroimage. 2009;44(2):489–501.
7. Filip P, Lungu OV, Manto M-U, Bareš M. Linking essential tremor to the cerebellum: physiological evidence. Cerebellum. 2016;15(6):774–80.
8. Marcián V, Filip P, Bareš M, Brázdil M. Cerebellar dysfunction and Ataxia in patients with epilepsy: coincidence, consequence, or cause? Tremor Hyperkinetic Mov. 2016;6:376. https://doi.org/10.7916/D8KH0NBT.
9. Bernard JA, Seidler RD. Moving forward: age effects on the cerebellum underlie cognitive and motor declines. Neurosci Biobehav Rev. 2014;42:193–207.
10. Raz N, Gunning-Dixon F, Head D, Williamson A, Acker JD. Age and sex differences in the cerebellum and the ventral pons: a prospective MR study of healthy adults. Am J Neuroradiol. 2001;22(6):1161–7.
11. Tang Y, Whitman GT, Lopez I, Baloh RW. Brain volume changes on longitudinal magnetic resonance imaging in normal older

people. J Neuroimaging. 2001;11(4):393–400. https://doi.org/10.1111/j.1552-6569.2001.tb00068.x.
12. Bernard JA, Seidler RD. Relationships between regional cerebellar volume and sensorimotor and cognitive function in young and older adults. Cerebellum. 2013;12(5):721–37. https://doi.org/10.1007/s12311-013-0481-z.
13. Bernard JA, Peltier SJ, Wiggins JL, Jaeggi SM, Buschkuehl M, Fling BW, et al. Disrupted cortico-cerebellar connectivity in older adults. NeuroImage. 2013;83:103–19. https://doi.org/10.1016/j.neuroimage.2013.06.042.
14. Ferreira LK, Busatto GF. Resting-state functional connectivity in normal brain aging. Neurosci Biobehav Rev. 2013;37(3):384–400. https://doi.org/10.1016/j.neubiorev.2013.01.017.
15. Tian L, Ma L, Wang L. Alterations of functional connectivities from early to middle adulthood: clues from multivariate pattern analysis of resting-state fMRI data. NeuroImage. 2016;129:389–400. https://doi.org/10.1016/j.neuroimage.2016.01.039.
16. Filip P, Lošák J, Kašpárek T, Vaníček J, Bareš M. Neural network of predictive motor timing in the context of gender differences. Neural Plast. 2016;2016:1–9.
17. Filip P, Gallea C, Lehéricy S, Bertasi E, Popa T, Mareček R, et al. Disruption in cerebellar and basal ganglia networks during a visuospatial task in cervical dystonia. Mov Disord. 2017;32(5):757–68.
18. Husárová I, Mikl M, Lungu OV, Mareček R, Vaníček J, Bareš M. Similar circuits but different connectivity patterns between the cerebellum, basal ganglia, and supplementary motor area in early Parkinson's disease patients and controls during predictive motor timing. J Neuroimaging. 2013;23(4):452–62.
19. Schmahmann JD, Sherman JC. The cerebellar cognitive affective syndrome. Brain J Neurol. 1998;121(4):561–79.
20. Diedrichsen J, Balsters JH, Flavell J, Cussans E, Ramnani N. A probabilistic MR atlas of the human cerebellum. NeuroImage. 2009;46(1):39–46. https://doi.org/10.1016/j.neuroimage.2009.01.045.
21. Diedrichsen J. A spatially unbiased atlas template of the human cerebellum. NeuroImage. 2006;33(1):127–38. https://doi.org/10.1016/j.neuroimage.2006.05.056.
22. Oldfield RC. The assessment and analysis of handedness: the Edinburgh inventory. Neuropsychologia. 1971;9(1):97–113.
23. Bares M, Lungu OV, Liu T, Waechter T, Gomez CM, Ashe J. The neural substrate of predictive motor timing in spinocerebellar ataxia. Cerebellum. 2011;10(2):233–44. https://doi.org/10.1007/s12311-010-0237-y.
24. Filip P, Lungu OV, Shaw DJ, Kasparek T, Bareš M. The mechanisms of movement control and time estimation in cervical dystonia patients. Neural Plast. 2013;2013:1–10.
25. Predictive motor timing and the cerebellar vermis in schizophrenia: an fMRI study | Schizophr Bull | Oxford Academic. https://academic.oup.com/schizophreniabulletin/article/42/6/1517/2399483. Accessed January 16, 2019.
26. Schuirmann DJ. A comparison of the two one-sided tests procedure and the power approach for assessing the equivalence of average bioavailability. J Pharmacokinet Biopharm. 1987;15(6):657–80.
27. Bares M, Lungu O, Liu T, Waechter T, Gomez CM, Ashe J. Impaired predictive motor timing in patients with cerebellar disorders. Exp Brain Res Exp. 2007;180(2):355–65.
28. Friston KJ, Buechel C, Fink GR, Morris J, Rolls E, Dolan RJ. Psychophysiological and modulatory interactions in neuroimaging. Neuroimage. 1997;6(3):218–29.
29. Eickhoff SB, Stephan KE, Mohlberg H, Grefkes C, Fink GR, Amunts K, et al. A new SPM toolbox for combining probabilistic cytoarchitectonic maps and functional imaging data. Neuroimage. 2005;25(4):1325–35.
30. Tzourio-Mazoyer N, Landeau B, Papathanassiou D, Crivello F, Etard O, Delcroix N, et al. Automated anatomical labeling of activations in SPM using a macroscopic anatomical parcellation of the MNI MRI single-subject brain. Neuroimage. 2002;15(1):273–89.
31. Wu T, Hallett M. The influence of normal human ageing on automatic movements. J Physiol. 2005;562(2):605–15. https://doi.org/10.1113/jphysiol.2004.076042.
32. Welford AT, Norris AH, Shock NW. Speed and accuracy of movement and their changes with age. Acta Psychol. 1969;30(C):3–15.
33. Jernigan TL, Archibald SL, Fennema-Notestine C, Gamst AC, Stout JC, Bonner J, et al. Effects of age on tissues and regions of the cerebrum and cerebellum. Neurobiol Aging. 2001;22(4):581–94. https://doi.org/10.1016/S0197-4580(01)00217-2.
34. Walhovd KB, Fjell AM, Reinvang I, Lundervold A, Dale AM, Eilertsen DE, et al. Effects of age on volumes of cortex, white matter and subcortical structures. Neurobiol Aging. 2005;26(9):1261–70. https://doi.org/10.1016/j.neurobiolaging.2005.05.020.
35. Sullivan EV, Deshmukh A, Desmond JE, Lim KO, Pfefferbaum A. Cerebellar volume decline in normal aging, alcoholism, and Korsakoff's syndrome: relation to ataxia. Neuropsychology. 2000;14(3):341–52. https://doi.org/10.1037//0894-4105.14.3.341.
36. Stoodley CJ. The cerebellum and cognition: evidence from functional imaging studies. Cerebellum. 2012;11(2):352–65.
37. Cabeza R. Hemispheric asymmetry reduction in older adults: the HAROLD model. Psychol Aging. 2002;17(1):85–100.
38. Ward NS, Frackowiak RSJ. Age-related changes in the neural correlates of motor performance. Brain J Neurol. 2003;126(0 4):873–88.
39. Taniwaki T, Okayama A, Yoshiura T, Togao O, Nakamura Y, Yamasaki T, et al. Age-related alterations of the functional interactions within the basal ganglia and cerebellar motor loops in vivo. NeuroImage. 2007;36(4):1263–76. https://doi.org/10.1016/j.neuroimage.2007.04.027.
40. Bo J, Peltier SJ, Noll DC, Seidler RD. Age differences in symbolic representations of motor sequence learning. Neurosci Lett. 2011;504(1):68–72. https://doi.org/10.1016/j.neulet.2011.08.060.
41. Driver J, Spence C. Multisensory perception: beyond modularity and convergence. Curr Biol. 2000;10(20):R731–5.
42. Schroeter ML, Zysset S, Kruggel F, Von Cramon DY. Age dependency of the hemodynamic response as measured by functional near-infrared spectroscopy. Neuroimage. 2003;19(3):555–64.
43. Huettel SA, Singerman JD, McCarthy G. The effects of aging upon the hemodynamic response measured by functional MRI. Neuroimage. 2001;13(1):161–75.
44. Park DC, Reuter-Lorenz P. The adaptive brain: aging and neurocognitive scaffolding. Annu Rev Psychol. 2009;60:173–96.
45. De Zeeuw CI, Ten Brinke MM. Motor learning and the cerebellum. Cold Spring Harb Perspect Biol. 2015;7(9):a021683.
46. Buckner RL, Krienen FM, Castellanos A, Diaz JC, Yeo BT. The organization of the human cerebellum estimated by intrinsic functional connectivity. J Neurophysiol. 2011;106(5):2322–45.